

Burning TADF Solids Reveals their Excitons' Mobility

Zhengyu Zhang,^a Arnaud Brosseau,^a Margaux Elie,^b Jean-Luc Renaud,^b Matthieu Hamel,^c
Sylvain Gaillard^b and Robert Bernard Pansu^{*,a,d}

^a Université Paris-Saclay, CNRS, ENS Paris-Saclay, PPSM UMR 8531, 91190 Gif-sur-Yvette, France.

^b LCMT, CNRS, UMR 6507, Normandie Université, 6 Bd. Maréchal Juin, F-14050 Caen, France.

^c Université Paris-Saclay, CEA, List, F-91120 Palaiseau, France; ORCID 0000-0002-3499-3966.

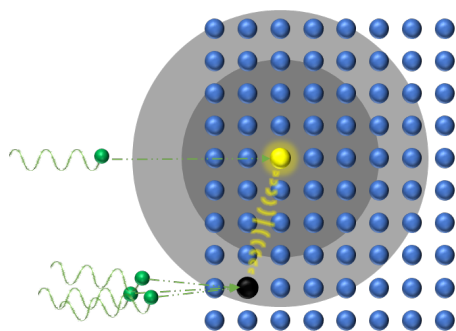
^d Université Paris-Saclay, CNRS, ENS Paris-Saclay, CentraleSupélec, LuMIn UMR9024 & Inst. d'Alembert FR3242, 91190 Gif-sur-Yvette, France.

HIGHLIGHTS The luminescence decays of solid samples are often complex due in part to the presence of defects. In the case of these TADF molecular solids, the analysis of the decays after the addition of defects provides the quenching distance of the triplet and singlet states.

ABSTRACT Nowadays, Thermally Activated Delayed Fluorescence (TADF) compounds have proven to be attractive for highly efficient optoelectronic devices as they can exploit both singlet and triplet excited states generated by charge recombinations that occur in such devices. However, quenching of excited states limits such benefits at high current densities. We have studied the quenching in the case of cationic copper(I) complexes coordinated by both *N*-heterolytic carbene (NHC) and 2,2'-dipyridylamine (dpa) ligands. Defects are created in their

crystals by a strong laser irradiation. Then we have investigated, by analysing their fluorescence decay as a function of temperature, the quenching mechanism and the exciton mobility. Using a time-resolved version of the Perrin's quenching model, we show that the quenching volume depends on temperature according to the singlet/triplet equilibrium. At room temperature, the singlet states are responsible for 75% of the quenching although they contribute for 2% to the excited states population. From the analysis of the decay curves, we show that the excitons are not mobile in the crystals and are quenched through Förster Resonant Energy Transfer (FRET).

GRAPHICAL ABSTRACT



KEYWORDS Luminescence decay, solid state luminescence, FRET, TADF, Perrin, exciton mobility, Copper complex luminescence.

INTRODUCTION

The luminescence decay in solids is always complex. This has been attributed to sample heterogeneity¹ and to distance-dependent quenching of the excited state by the defects or impurities². Local environment heterogeneity is often dominated by the presence of a few defects close to the excited state. The decay without quenchers is significantly different from that with one quencher. To the opposite, in solution, the Brownian motion averages out distances and numbers of quenchers before the emission of the photon. In solution, all emitters

can be considered to have the same environment and the same lifetime. Thus, it is often assumed that the lifetimes are associated with species. In solid, even if crystallized samples are quite clean and neat, the population of the excited states is a mixture of excitons with zero, one, two, ... a few defects with different quenching rates. This multiplicity of lifetimes explains why nowadays, decays in solid are often overlooked. In solid, the description of the fluorescence requires the calculation of the numbers of defects and their corresponding distribution. The calculation of the number of defects that are within the quenching volumes around the excited states is known as the Perrin model.^{3,4,5} In particular, the fraction of the excitons that have no quenchers in their surroundings (Fig. 1a), have an exponential decay with the longest lifetime and was expressed by F. Perrin as:³

$$F_{pur} = \exp\left(-[Q]V_Q(T)\right), \quad (1)$$

where $[Q]$ is the density of the quenching defects and $V_Q(T)$ is the quenching volume. In this contribution, we shall measure the number of defects within the quenching volume (Fig. 1b) and determine the quenching process from the analysis of the shape of the fluorescence decay curves. For that we create defects by burning the sample at high laser fluences.

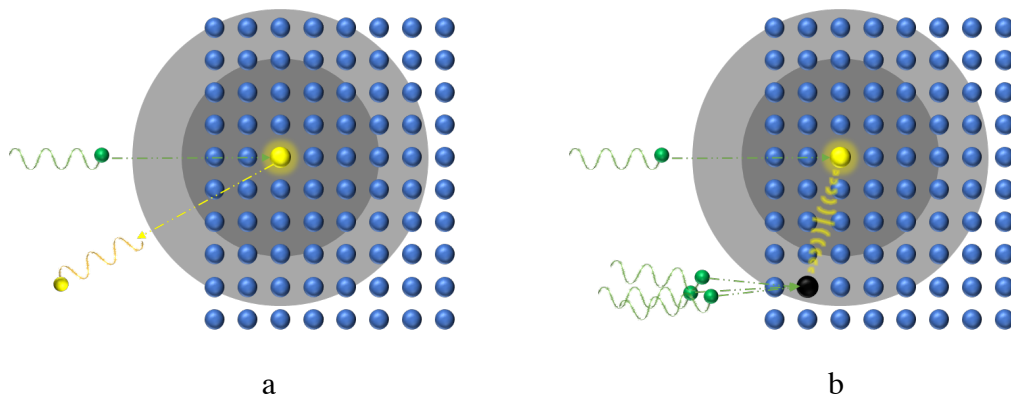


Figure 1. *Perrin's quenching model. (a) An exciton with no defect in the quenching volume. The non-quenched excitons have an exponential decay. (b) When a defect is created by light within the quenching volume of an exciton, the exciton will be quenched. The lighter grey sphere*

around the exciton represents the Förster volume for the singlet state and the darker grey sphere for the triplet state.

Electroluminescence, used in OLED (Organic Light Emitting Diode) or LEC (Light-Emitting Electrochemical Cell) technologies, is an emission of light resulting from the excited state, generated by the recombination of an electron and a hole in the emitting layer, of the emissive compound. However, spin statistics implies that 75% of the electrically generated pairs are triplets, which have most of the time a low luminescence yield for the majority of organic compounds. Compounds that exhibit a delayed fluorescence after thermal activation of the triplets (TADF) can also convert efficiently triplet states into light.⁶ Among the known TADF emitters, copper(I) complexes are one of the most attractive.^{7,8,9} It is noteworthy that the highest yields in OLEDs, although reaching ~100%, are achieved at low current densities only, whereas above 100 mA/cm², this yield is reduced and a roll-off of the luminescence is observed because of the quenching of excited states by charges or by their mutual annihilations.¹⁰ The operation of OLEDs at high luminescence thus requires the control of these losses.

In this paper, we study the quenching of [Cu(IPr)(dpa)][PF₆] (IPr: 1,3-bis-(2,6-diisopropylphenyl)imidazol-2-ylidene; dpa: 2,2'-dipyridylamine), shown on Fig. 2, in its crystalline form¹¹ (see experimental section and the paragraph a of the Supplementary Information (SIa)). Indeed, we have reported a family of

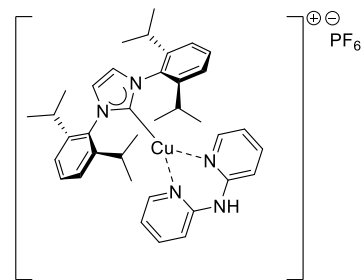


Fig. 2 [Cu(IPr)(dpa)][PF₆].

[Cu(NHC)(N[^]N)]⁺ complexes (NHC = *N*-Heterocyclic Carbene, and N[^]N = bridged bis-pyridyl derivatives) that exhibit a TADF behavior and some of them have been successfully applied in LEC devices.^{12,13,14} Even if the [Cu(IPr)(dpa)][PF₆] complex was not the best candidate in such technology, due to relatively low photo-stability, its photophysics is representative of this family (see paragraph b of the Supplementary Information (SIb) on equivalent results on a second member of the family [Cu(IPr)(³Me dpa)][PF₆]). We have made profit of this photo-

degradation to investigate the mobility of the excitons and the quenching mechanism in this solid.

In TADF materials, the excited states equilibrate between the singlets and triplets according to equation (2):¹⁵

$$R(T) = \frac{[S_1]}{[T_1]} = \frac{\phi_{isc}}{3} \exp\left(-\frac{\Delta E_{ST}}{kT}\right) \quad (2)$$

where $[S_1]$ and $[T_1]$ are the concentrations of singlets and triplets, ΔE_{ST} is the energy difference between singlet and triplet states per luminescence site, k is the Boltzmann constant, T is the temperature. $\phi_{isc} = \frac{k_{isc}}{k_{isc}+k_f+k_{nr}+k_{FRET}}$ is the yield of the intersystem conversion to the triplet state compared to the other deactivation rates of the singlet. ϕ_{isc} is 1 when the intersystem conversion is fast compared to the decay rate of singlet state.¹⁶

This temperature dependence of the singlet/triplet equilibrium allows the observation of the impact of the nature of the excited states on the quenching, in the same TADF sample, with the same concentration and distribution of defects. From equation (1) a measure and an analysis of the quenching volume as a function of temperature is possible. We show that the Förster energy transfer is the path of the quenching of both triplet and singlet states but with a larger quenching volume in the case of singlets (2.4 times larger for $[\text{Cu}(\text{IPr})(\text{dpa})][\text{PF}_6]$ crystals). The dynamics of the quenching in $[\text{Cu}(\text{IPr})(\text{dpa})][\text{PF}_6]$ crystals show that excitons are trapped, which prevent the triplet-triplet and singlet-singlet annihilations and limit the quenching by charge carriers.

MATERIAL AND METHODS

Crystals of $[\text{Cu}(\text{IPr})(\text{dpa})][\text{PF}_6]$ were obtained from a slow gas diffusion of hexane into a chloroform solution of the copper complex. Crystals were then crunched to prepare crystals with thickness smaller than the extinction length of the laser into individual particle.¹⁷ They were then dispersed into a KBr powder at a dispersion of 5% by weight to form a homogeneous sample that fits with the laser beam diameter. The mixture was inserted into an Oxford Instrument cryostat and the temperature was controlled by a nitrogen gas flow between 77 K

and 310 K. The sample was excited with the third harmonic of a NdYAG laser Surelite from Continuum. The energy was 2 mJ per pulse over an area of 0.25 cm². The pulse duration was 5 ns and the repetition rate was 10 Hz. The luminescence was collected at 90° and analyzed with a transient absorption setup, LP920 from Edinburgh Instrument at 500±2.5 nm. The setup was previously described.¹⁸

RESULTS AND DISCUSSION

Generation of defects

We think that the photo-transformation of luminescent molecules in solids (burning) is a suitable way to probe the mobility and the quenching volume of the excitons. In the excited state, molecules have an excess of energy that can lead to their destruction and thus the formation of photoproducts that will quench the luminescence. Consequently, a [Cu(IPr)(dpa)][PF₆] sample was bleached by strong laser irradiations (80 pulses of 8 mJ/cm² of the third harmonic of a NdYAG laser for each measurement) to create quenchers in the crystals. This is ten times more than the power typically used to study such samples.¹¹

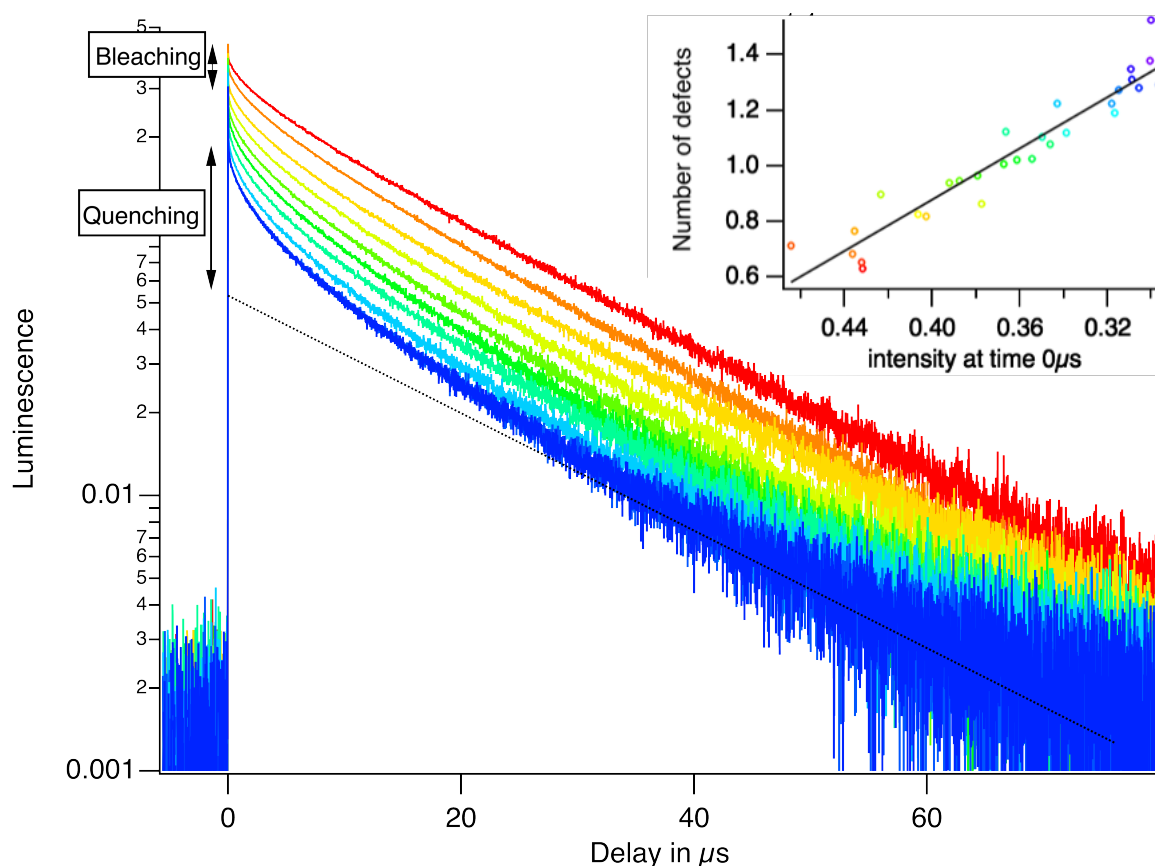


Figure 3. Luminescence decay curves recorded during the bleaching of $[\text{Cu}(\text{IPr})(\text{dpa})][\text{PF}_6]$ crystals at room temperature. From red to blue, the number of laser shots was 240 between each curved displayed. The drop of the time zero intensities reflects the destruction of the luminescent sites. The increase of the initial decay rates reflects the creation of quenchers as photoproducts of the bleaching. The long-lived population corresponds to excitons far away from any quencher. Their number decreases as the number of quenchers increases. The average number of quenchers per luminescent site, given by Perrin's model, is displayed on the inset as a function of the loss of the initial intensity.

The bleaching of the sample is seen in Figure 3 from the drop of the fluorescence at time $0 \mu\text{s}$. The delayed fluorescence starts after this initial fluorescence. The creation of defects can be observed from the increase of the initial decay rate coefficient $d\ln(I(t))/dt$ of the

luminescence. The presence of the non-quenched excitons is seen in the persistence of the excitons with a constant long lifetime of $19 \pm 0.2 \mu\text{s}$. The decays have been analyzed according to the model of quenching by a few quenchers.^{3,4,19} The Principal Component Analysis test of the proportionality of the decay rate coefficient $d\ln(I(t))/dt$ with the quencher concentration and the quality of the description based on the data obtained by Perrin's model are shown in Fig. S.3, Fig. S.4 and Fig. S.10 in the SI. The proportionality of the decay rate with the quencher concentration is a very general property.⁵ More significant is the observation of a safe population with a constant lifetime during the "burning process". From the fraction of the safe population, the number of quenchers in the quenching volume around the excitons is extracted using equation (1). The number of quenchers $\Delta\text{Ln}(I_{\text{long}})$ versus the loss of the initial intensity was plotted on the inset of Figure 3. The proportionality shows a constant yield for the photo-production of quenchers at the expense of the original molecules. The complex decay observed before bleaching can be ascribed to the presence of some quenchers in the neat sample with the same quenching rate as the photoproducts (see SI(g)). In some cases, a cautious recrystallization leads to crystals without fast initial decay (see Fig. S8).

Below 240 K, the burning of the sample by the laser is not efficient (see SI(o)). Therefore, the "burning process" cannot be operated at cryogenic temperatures. But still the effect of temperature can be studied on partially burned samples.

The singlet–triplet equilibrium

Figure 4 shows the luminescence decays recorded as a function of temperature. 20 Laser shots were used to record the decays in order to limit the bleaching.

The common lifetime of the excited states depends on temperature and is given by:⁸

$$\frac{1}{\tau} = \frac{1/\tau_T + R(T)/\tau_S}{1+R(T)}, \quad (3)$$

where τ_T is the triplet decay time, τ_S is the singlet decay time, $R(T)$ is the ratio of singlets to triplets as a function of temperature in equation (2).

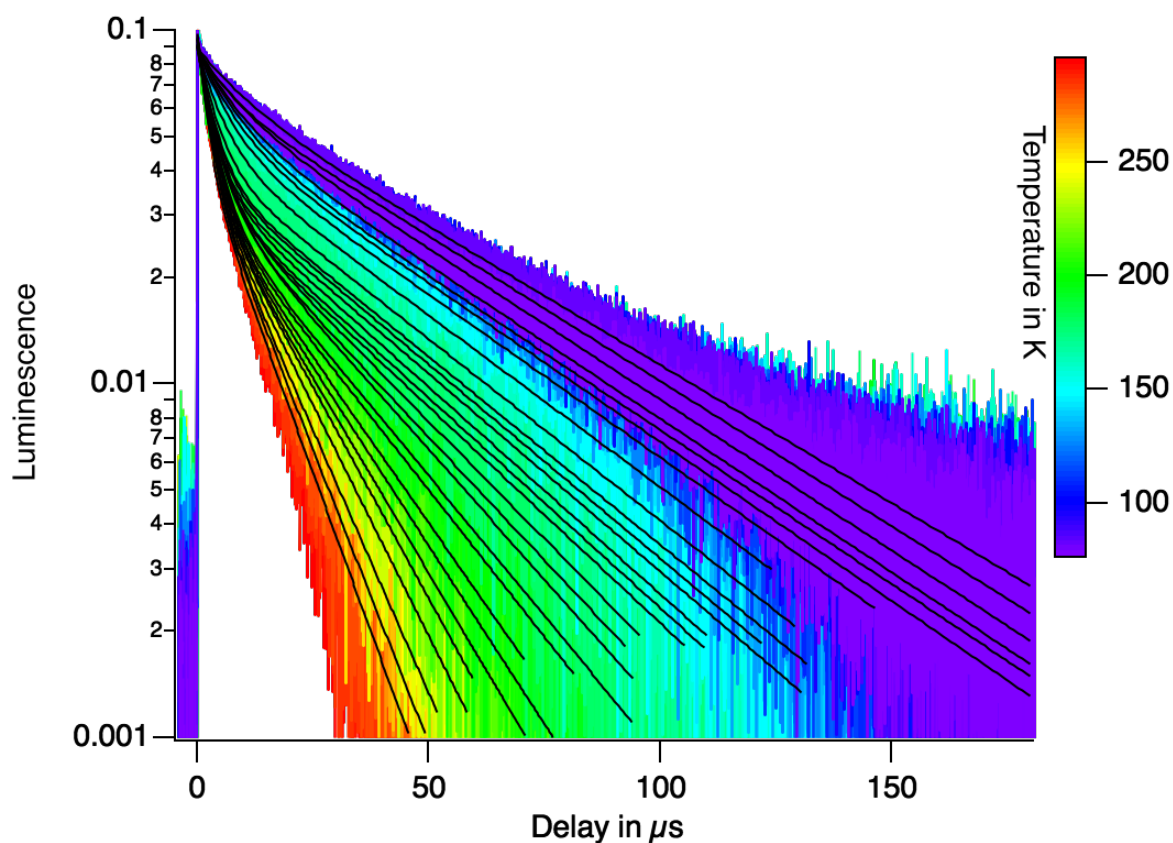


Figure 4. The fluorescence decays of $[\text{Cu}(\text{IPr})(\text{dpa})][\text{PF}_6]$ crystals as a function of temperature. The decays were fitted as bi-exponentials. The long-lived decay is from the unquenched population. The fluorescence lifetime decreases with temperature because of the thermal activation of triplets into singlets. The fast decay at short time comes from the quenched population. From the amplitude of the fluorescence drop due to this fast component, we can measure the number of quenchers in the quenching volume around the excited states using equation (1).

The decays at all temperatures are complex and multi-exponentially shaped. However, the long-lived population gives a well-defined exponential contribution to the luminescence decay. A biexponential fit allows us to extract safely the lifetime and the fraction of the long component. The long-lived population is the fraction of the excitons that are safe from quenching (

Figure 1).

The decay rates of the long component at different temperatures are represented in Figure 5, as well as the number of quenchers derived from the long component's relative contributions (equation (1)).

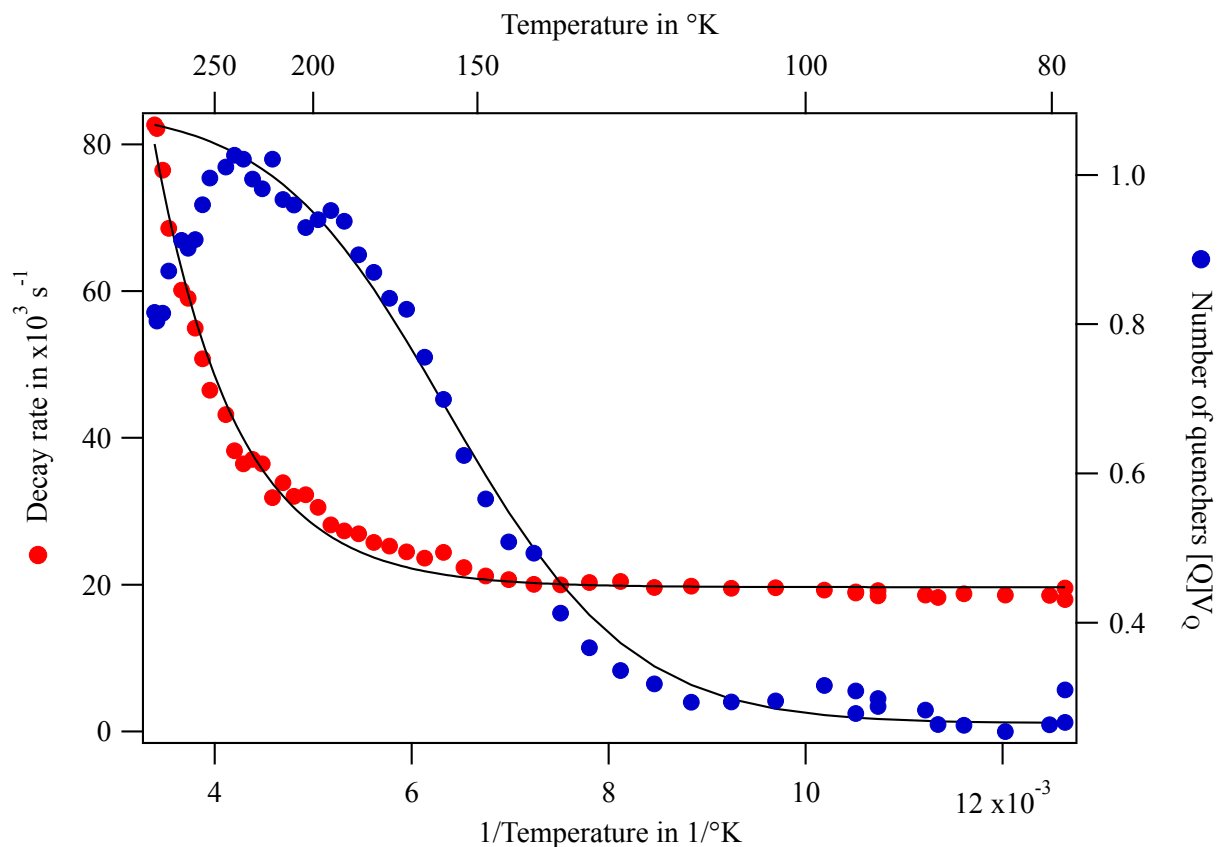


Figure 5. The decay rates of the long component at different temperatures and the numbers of quenchers derived from the long component's relative contributions. The decay rate of the unquenched population depends on temperature because of the Boltzmann equilibrium between the singlet and triplet states. From that, the energy difference between the two states is measured to be 10 kJ/mol. The average number of the quenchers in the quenching volume per exciton rises between room temperature and 240 K. We hypothesize that the burning process was still present at these temperatures. Below 240 K, there is no more burning; the average quenching volume decreases with the singlet state population.

[Cu(IPr)(dpa)][PF₆]'s lifetime dependence with temperature in crystals was fitted by equation (3), from which three values were extracted: the singlet lifetime, the triplet lifetime at low

temperature and ΔE_{ST} , the energy gap between the singlet and triplet states of [Cu(IPr)(dpa)][PF₆]. These values are :

$$\tau_s = 13 \pm 1 \text{ ns};$$

$$\tau_T = 52.8 \pm 0.2 \mu\text{s};$$

$$\Delta E_{ST}/k = 1210 \pm 10 \text{ K}; N_A \Delta E_{ST} = 10.0 \pm 0.1 \text{ kJ/mol}.$$

ϕ_{isc} was set equal to 1. The singlet/triplet splitting agrees with the calculations according to the time-dependent density functional theory.¹² At 77 K, the probability for the luminescent site to be a singlet exciton is only 10⁻⁸ whereas at room temperature [Cu(IPr)(dpa)][PF₆] spends 2% of its time as a singlet. The singlet will induce an increased quenching through a faster FRET.

The size of the quenching volume

Figure 5 shows the relationship between the quenching volume and the temperature. In this experiment, only the number of quenchers n_Q in the quenching volume V_Q ($n_Q = [Q]V_Q$, where $[Q]$ is the density of quenchers) were measured and not directly V_Q . The quencher concentration is constant, thus the higher number of quenchers involved in the quenching reflects the increase of the quenching volume. At low temperature, the excited TADF unit spends most of its time as a triplet. At room temperature, the singlet state contributes as well. We shall assume a FRET for both the triplet state and the singlet state.^{2,20} Whatever the quenching mechanism, we want to express the presence of a characteristic distance for that mechanism. To assume a FRET for both the singlet and triplet state makes the equation easier to handle. Let's define the quenching volume V_Q of a TADF compound by the distance at which the transfer rate coefficient to the quencher equals the decay rate coefficient of the non-quenched population.²¹ The quenching rate is the sum of the rates by the two forms of the excited state weighted by their respective probabilities. If V_{QT} and V_{QS} are respectively the quenching volumes of the triplet and singlet, V_Q will verify equation (4):

$$\frac{1/\tau_T (V_{QT}/V_Q)^2}{1+R(T)} + \frac{1/\tau_S (V_{QS}/V_Q)^2 R(T)}{1+R(T)} = \frac{1}{\tau} = \frac{1/\tau_T + R(T)/\tau_S}{1+R(T)}, \quad (4)$$

which leads to express V_Q^2 as:

$$V_Q^2 = \frac{V_{QT}^2/\tau_T + R(T) V_{QS}^2/\tau_S}{1/\tau_T + R(T)/\tau_S}. \quad (5)$$

The experimental values and the fit according to equation (5) are presented on Figure 5. The factors $\Delta E_{ST}/k$, τ_S , τ_T are in common in equation (4) and (5) and have been obtained by a global fit of the two sets of data of Figure 5. The intersystem crossing yield ϕ_{isc} was set to 1 for the analysis of the non-quenched population (equation 3) and found to be 0.15 for the quenched population (equation 5) (See SI(l)). This might be because the quenching competes with the intersystem crossing and reduces the ϕ_{isc} yield for the quenched population. From the fit by equation (5), two extra values can be extracted, namely the number of quenchers in the triplet quenching volume at low temperature (0.46) and the number of quenchers in the singlet quenching volume (1.1). These two values can be read on Figure 5 from the values of the plateau at low and room temperatures. Due to the difference in the weighting factors of equation (3) and (5), a minority of singlet states (2%) at room temperature are responsible for most of the quenching (75%). On Figure 5 an increase of the number of quenchers between room temperature and 240 K is seen that is not described by our model. It could be due to the burning of the sample during the measurement process. It cannot be due to a quenching of the triplets through a Dexter electron exchange (See SI(m)).

The quenching dynamics

Equation (6) was proposed by Millar *et al.* for the fluorescence decay of a quenched population and it has been tested for solutions:²²

$$\ln\left(\frac{I(t)}{I_0}\right) = -k_F t - [Q] \left(4\pi D r_f t + G\pi^2 R_0^3 \sqrt{k_F t} \right), \quad (6)$$

Importantly, the $R_0^3\sqrt{k_F t}$ is due to the distance dependence of the FRET quenching in three dimensions.^{23,24} This term is obtained as an approximation for short times of the more complex equation using the Perrin model and neglects the existence of a non-quenched population.²⁰ The term linear with time, $4\pi D r_f$, describes the diffusion of the excitons and quenchers. In solids, the diffusion can be due to a hopping of the excitation from site to site. As a diffusion rate, it must be positive.

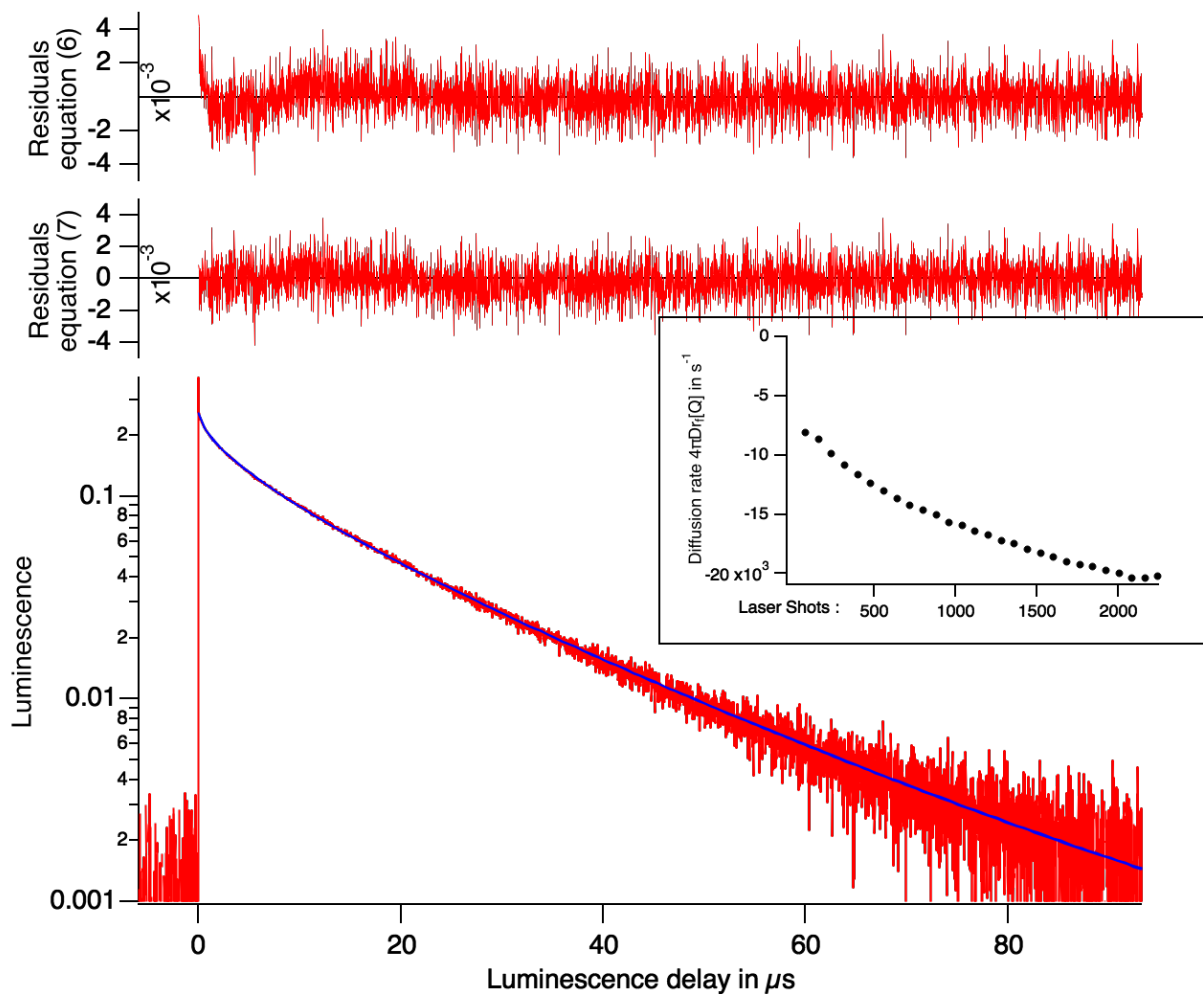


Figure 6. A global fit of the decays during the bleaching has been performed with Millar *et al.*'s equation (6) and our equation (7). Record number 11 is shown as an example. The residuals are displayed on the top plot for equation (6) and on lower plot for equation (7). The diffusion term is plotted on the inset.

Equation (6) including an offset term for the adjustment of the baseline can be used to fit the data. A global fit of the family of decays produced during the bleaching experiment of Figure 3, where k_F and the ratio $GR_o^3/4Dr_f\sqrt{\pi k_F}$ are the common parameters. The results are presented in Table 1. The diffusion rate $4\pi Dr_f[Q]$ is free to change among successive curves. The result is shown on Figure 6 for the eleventh measurement. Residuals are on the top plot and all residuals can be found in SI(k). The fit is numerically satisfying, but with a negative value of $-14650 \pm 37 \text{ s}^{-1}$ for the diffusion rate. This negative diffusion rate becomes more pronounced as the concentration of quenchers is increased as shown on the inset of Figure 6.

Table 1 Results of the global fit, by Millar's model and by Perrin's model, of the decays collected during the burning.

Millar eq. (6)			Perrin eq. (7)		
$-k_F t - [Q] \left(4\pi D r_f t + G \pi^2 R_o^3 \sqrt{k_F t} \right)$			$-k_F t - V_Q [Q] \left\{ 1 - \exp \left(-\sqrt{\pi k_Q t} \right) \right\}$		
$k_F \text{ s}^{-1}$	Fix	46760.4	$k_F \text{ s}^{-1}$	Common	25500 ± 92
$GR_o^3/4Dr_f\sqrt{\pi k_F}$	Common	$17 \pm 1 \cdot 10^{-3}$	$k_Q \text{ s}^{-1}$	Common	13200 ± 400
$4\pi Dr_f[Q]$	Free		$V_Q[Q]$	Free	

From the non-positive values of the diffusion coefficient, we assume the absence of diffusion for the excitons and the quenchers in $[\text{Cu}(\text{IPr})(\text{dpa})][\text{PF}_6]$ crystals at low temperatures. Trapped excitons will be less sensitive to singlet-singlet and triplet-triplet annihilations, which is attractive for lightening applications. However, the strictly negative value of the diffusion coefficient obtained from the fit is disturbing. Such specific time dependence of the quenching rate may come from some specific quencher/exciton distribution curve in the case of $[\text{Cu}(\text{IPr})(\text{dpa})][\text{PF}_6]$ crystals. But Equation (6) neglects the presence of an unquenched population. From the presence of an unquenched population, both at room temperature and at liquid nitrogen temperature, we know that we have only a few quenchers per exciton: less than 1.4 quenchers per exciton are seen in Figure 3.

Thus, different populations of luminescent sites with no, one, two, ..., a few quenchers can be envisaged, leading to express the total decay as:

$$\ln\left(\frac{I(t)}{I_0}\right) = -k_F t - V_Q[Q]\{1 - \exp(-\sqrt{\pi k_Q t})\}, \quad (7)$$

where $V_Q[Q]$ is the number of quenchers in the Perrin volume. $\{1 - \exp(f(t))\}$ term comes from the distribution of the number of quenchers.^{4,5} $\exp(-\sqrt{\pi k_Q t})$ is the decay of an ensemble of luminescent sites with only one FRET quencher. The decay with equation (7) was fitted as shown on Figure 6 and residuals are on the lower plot. The residuals are better than those of equation (6) (see SI(e) for the global residues), but more importantly now the presence of quenchers increases the decay rate as expected. The success of the two models confirms that the complexity of the luminescence decay of such TADF copper complexes is due to the presence of a few defects per luminescent center. The contribution of the population without quencher to the late fluorescence is clearly seen from the data. The presence of this population is often overlooked in solid-state luminescence studies where the short time validity of approximate equations is favored over the late time validity.²⁵ Both models conclude to the immobility of the luminescent centers in the solid which support that this $[\text{Cu}(\text{IPr})(\text{dpa})][\text{PF}_6]$ complex family is of interest for lightning applications.

CONCLUSION

The decay of the fluorescence of solids is always complex, but important pieces of information were extracted from the burning of TADF $[\text{Cu}(\text{IPr})(\text{dpa})][\text{PF}_6]$ crystals. In addition to the short component corresponding to the direct fluorescence and the long component ascribed to the thermally activated delayed fluorescence, we have observed and studied an intermediate component that we attribute to the presence of defects in the solids. Burning the sample at high laser fluence amplifies that intermediate component. We successfully analyze the decays observed as due to the presence of a few quenchers per exciton, using an extension to the time-resolved luminescence of the statistical analysis done by Perrin. At room

temperature, the quenching rate coefficient is a square root of time. This is that of a FRET from the fixed exciton to a fixed trap. From the analysis of the fraction of non-quenched excitons, the number of quenchers within the FRET distance has been extracted. This fraction that exponentially depends on the quencher concentration can only be measured using spectroscopic techniques with a dynamic range of a few orders of magnitude. The same analysis could be performed using light pulses or electrical pulses in OLEDs for the determination of the local number of defects.

With TADF compounds, by changing the temperature we can change the nature of the excitons. We have assumed a FRET for the triplet state quenching. This enables us to define a quenching volume and compare its values with our model. The analysis of the quenching extant offers a second way to measure ΔE_{ST} , the energy gap between the singlet and the triplet states. In the case of [Cu(IPr)(dpa)][PF₆] complex, since the critical temperature at which the quenching shifts (160 K) is more accessible than the critical temperature at which the lifetime shifts, a better measurement of the energy gap between singlet and triplet can be obtained. Because of the difference between the two critical temperatures, it appears that, at room temperature, even if the singlet states have a very short lifetime and contribute only to 2% the excited states, they dominate the quenching and the quenching dynamics.

As a conclusion, this study shows that a few defects in an almost perfect sample complicate the photo-physics of solids, but they can be used to gain a better knowledge of the excitons behavior. Adding defects by a laser treatment is a useful way to interrogate the photophysics of a solid sample.

Supporting Information

Content:

- a) Materials
- b) Burning [Cu(IPr)(³Me_edpa)][PF₆] at high laser fluence
- c) The binomial distribution of the number of quenchers around emitters

- d) Principle Component Analysis
- e) Building of the decay rates
- f) The quencher free decay
- g) Temperature dependence of a defect-less sample
- h) The production yield of the quenchers
- i) The shape of the quenching rates
- j) The global fit of the luminescence decays
- k) Equation for the temperature dependence of the quenching volume
- l) The global fit
- m) Temperature dependence of the bleaching

ACKNOWLEDGMENT

This work is supported by the CNRS (Centre National de la Recherche Scientifique), the Agence Nationale de Recherche as part of the NESSYNED project (contract ANR-15-CE39-0006). Zhengyu Zhang is grateful for support from the Ecole doctorale INTERFACES of University Paris Saclay. We thanks the “Région Basse-Normandie” for their funding (M.E.). SG thanks Johnson Matthey for the gift of metals.

REFERENCES

¹ J Macklin, J. J.; Trautman, J. K.; Harris, T. D.; Brus, L. E., Imaging and time resolved spectroscopy of single molecules at an interface. *Science* **1996**, 272, 255-258. DOI: [10.1126/science.272.5259.255](https://doi.org/10.1126/science.272.5259.255)

-
- ² Förster, T., 10th Spiers Memorial Lecture. Transfer mechanisms of electronic excitation. *Discuss. Faraday Soc.* **1959**, *27*, 7-17. DOI: 10.1039/df9592700007
- ³ Perrin, F., Loi de décroissance du pouvoir fluorescent en fonction de la concentration. *Comptes rendus de l'académie des sciences* **1924**, *178*, 1978-1980. <http://visualiseur.bnf.fr/Visualiseur?Destination=Gallica&O=NUMM-3131>
- ⁴ Blumen, A.; Manz, J., On the concentration and time dependence of the energy transfer to randomly distributed acceptors. *J. Chem. Phys.* **1979**, *71*, 4694-4702. DOI: 10.1063/1.438253
- ⁵ Hartmann, L.; Kumar, A.; Welker, M.; Fiore, A.; Julien-Rabant, C.; Gromova, M.; Bardet, M.; Reiss, P.; Baxter, P. N. W.; Chandezon, F.; Pansu, R. B., Quenching Dynamics in CdSe Nanoparticles: Surface Induced Defects upon Dilution. *ACS Nano* **2012**, *6*, 9033–9041. DOI: 10.1021/nn303150j
- ⁶ Uoyama, H.; Goushi, K.; Shizu, K.; Nomura, H.; Adachi, C., Highly efficient organic light-emitting diodes from delayed fluorescence. *Nature* **2012**, *492*, 234-238. DOI: 10.1038/nature11687
- ⁷ B. E. Housecroft, E. C. Constable, *J. Mater. Chem. C*, 2022, DOI: 10.1039/d1tc04028f.
- ⁸ C. Mahoro, G. U., Fernandez-Cestau, J., Renaud, J.-L., Coto, P. B., Costa, R. D., Gaillard, S. *Adv. Optical Mater.* 2020, 2000260. DOI: 10.1002/adom.202000260.
- ⁹ Leitl, M. J.; Krylova, V. A.; Djurovich, P. I.; Thompson, M. E.; Yersin, H., Phosphorescence versus thermally activated delayed fluorescence. Controlling singlet-triplet splitting in brightly emitting and sublimable Cu(I) compounds. *J. Am. Chem. Soc.* **2014**, *136*, 16032-16038. DOI: 10.1021/ja508155x

¹⁰ Sandanayaka, A. S. D.; Yoshida, K.; Matsushima, T.; Adachi, C., Exciton Quenching Behavior of Thermally Activated Delayed Fluorescence Molecules by Charge Carriers. *The Journal of Physical Chemistry C* **2015**, *119* (14), 7631-7636. DOI: 10.1021/acs.jpcc.5b01314

¹¹ Marion, R.; Sguerra, F.; Sauvageot, E.; Lohier, J.-F.; Daniellou, R.; Renaud, J.-L.; Linares, M.; Hamel, M.; Gaillard S. NHC Copper(I) Complexes Bearing Dipyriddyamine Ligands: Synthesis, Structural, and Photoluminescent Studies. *Inorg. Chem.* **2014**, *53*, 9181-9191. DOI: /10.1021/ic501230m

¹² Elie, M.; Sguerra, F.; Di Meo, F.; Weber, M. D.; Marion, R.; Grimault, A.; Lohier, J.-F.; Stallivieri, A.; Brosseau, A.; Pansu, R. B.; Renaud, J.-L.; Costa, R. D.; Linares, M.; Hamel, M.; Gaillard, S., Designing NHC-Copper(I) Dipyriddyamine Complexes for Blue Light-Emitting Electrochemical Cells. *ACS Appl. Mater. & Inter.* **2016**, *8*, 14678-14691. DOI: 10.1021/acsami.6b04647

¹³ Elie, M.; Weber, M. D.; Di Meo, F.; Sguerra, F.; Lohier, J.-F.; Pansu, R. B.; Renaud, J.-L.; Hamel, M.; Linares, M.; Costa, R. D.; Gaillard, S., Role of the bridging group in bis-pyridyl ligands: Enhancing both photo- and electro-luminescent features of cationic (IPr)Cu(I) complexes. *Chem. Eur. J.* **2017**, *23*, 16328-16337. DOI: 10.1002/chem.201703270

¹⁴ Leitzl, M. J.; Zink, D. M.; Schinabeck, A.; Baumann, T.; Volz, D.; Yersin, H., Copper(I) Complexes for Thermally Activated Delayed Fluorescence: From Photophysical to Device Properties. *Topics in Curr. Chemi.* **2016**, *374*, 25. DOI: 10.1007/s41061-016-0019-1

¹⁵ Graves, D.; Jankus, V.; Dias, F. B.; Monkman, A., Photophysical Investigation of the Thermally Activated Delayed Emission from Films of m-MTDATA:PBD Exciplex. *Adv. Funct. Mater.* **2014**, *24*, 2343-2351. DOI: 10.1002/adfm.201303389

¹⁶ Etherington, M. K.; Gibson, J.; Higginbotham, H. F.; Penfold, T. J.; Monkman, A. P., Revealing the spin-vibronic coupling mechanism of thermally activated delayed fluorescence. *Nat. Commun* **2016**, *7*, 13680. DOI: 10.1038/ncomms13680

¹⁷ Laurent, G.; Ha-Duong, N. T.; Méallet-Renault, R.; Pansu, R. B., Effect of size and light power on the fluorescence yield of rubrene nanocrystals. In *Nanophotonics: Integrating Photochemistry, Optics, and Nano/BioMaterials Studies*, Masuhara, H.; Kawata, S., Eds. Elsevier: Amsterdam, 2004; pp 89-102.

¹⁸ Wrona-Piotrowicz, A.; Zakrzewski, J.; Metivier, R.; Brosseau, A.; Makal, A.; Wozniak, K., Efficient synthesis of pyrene-1-carbothioamides and carboxamides. Tunable solid-state fluorescence of pyrene-1-carboxamides. *RSC Advances* **2014**, *4* (99), 56003-56012. DOI:10.1039/c4ra07045c

¹⁹ Blumen, A., On the direct energy transfer via exchange to randomly distributed acceptors. *J. Chem. Phys.* **1980**, *72*, 2632. DOI: /10.1063/1.439408

²⁰ Charbonniere, L. J.; Hildebrandt, N.; Ziessel, R. F.; Loehmannsroeben, H. G., Lanthanides to quantum dots resonance energy transfer in time-resolved fluoro-immunoassays and luminescence microscopy. *J. Am. Chem. Soc.* **2006**, *128* , 12800-12809. DOI: 10.1021/ja062693a

²¹ Blumen, A.; Klafter, J., Quenching of luminescence by non-radiative tunnelling. *Philosophical Magazine Part B* **1983**, *47* (2), L5-L8. DOI: 10.1080/13642812.1983.9728435

²² Millar, D. P.; Robbins, R. J.; Zewail, A. H., Picosecond dynamics of electronic energy transfer in condensed phases. *J. Chem. Phys.* **1981**, *75*, 3649-59. DOI:10.1063/1.442529

²³ Gosele, U.; Hauser, M.; Klein, U. K. A.; Frey, R., Diffusion and long-range energy transfer. *Chem. Phys. Letters* **1975**, *34*, 519-522. DOI:10.1016/0009-2614(75)85553-9

²⁴ Heisel, F.; Mieke, J. A., Intermolecular transfer and quenching of electronic excitation energy in fluid solutions: Interpretation of experimental data with a diffusion model including distance dependent interaction. *J. Chem. Phys.* **1982**, *77*. DOI: 10.1063/1.444128

²⁵ Murata, S.; Tachiya, M., Refined Perrin equation for the analysis of fluorescence quenching by electron transfer. *Chem. Phys. Letters* **1992**, *194*, 347-350. DOI: 10.1016/0009-2614(92)86062-m